# MEASUREMENT OF LOW ENERGY $e^+e^-$ INTERACTIONS AT BABAR WITH INITIAL STATE RADIATION*

Fabio Anulli

Lab. Nazionali di Frascati dell'INFN
via E. Fermi 40, 00044 Frascati (Rm), Italy
on behalf of the BaBar Collaboration

*(Received November 2, 2005)*

The status of the analysis of $e^+e^-$ annihilation using the radiative return technique at BaBar is presented. Cross sections for the processes $e^+e^- \to \pi^+\pi^-\pi^0$, $\pi^+\pi^-\pi^+\pi^-$, $\pi^+\pi^-K^+K^-$, $K^+K^-K^+K^-$, $3(\pi^+\pi^-)$, $\pi^0\pi^0 2(\pi^+\pi^-)$, $K^+K^-2(\pi^+\pi^-)$ and $p\bar{p}$ are measured in the energy range from threshold up to 4.5 GeV. Studies on resonant structures involved in these processes have been performed. We present also new precise measurements of the effective proton form factor and of the ratio of the electric to magnetic proton form factor, $|G_{\rm E}/G_{\rm M}|$. In addition, the $J/\psi$ and $\psi(2S)$ branching fractions to all these final states have been measured.

PACS numbers: 13.40.Ks, 13.66.Bc

## 1. Introduction

Initial state radiation (ISR) processes can be effectively used to measure $e^+e^-$ annihilation at high luminosity $e^+e^-$ storage rings, such as the $B$-factory PEP-II [1–3]. A large mass range is accessible in a single experiment, contrary to the case with fixed energy colliders, which are optimized only in a limited region. In addition, the broad-band coverage may result also in greater control of systematic effects because only one experimental setup is involved.

The ISR physics program consists mainly on light hadron spectroscopy and measurement of the ratio $R = \sigma(e^+e^- \to \text{hadrons})/\sigma(e^+e^- \to \mu^+\mu^-)$, which provides the experimental input to dispersion integrals for computation of the hadronic contribution to the theoretical estimation of the muon anomalous magnetic moment, $a_\mu = (g-2)_\mu/2$ and of the running of the electromagnetic coupling to the $Z$ pole, $\alpha(M_Z^2)$.

* Presented at the XXIX International Conference of Theoretical Physics, "Matter to the Deepest", Ustroń, Poland, September 8–14, 2005.

The ISR cross section for a particular final state $f$ is related to the cross section for the direct annihilation $e^+e^- \to f$ through

$$\frac{d\sigma(s,x)}{dx} = W(s,x)\ \sigma_f(s')\,, \qquad s' = s(1-x)\,, \tag{1}$$

where $x = 2E_\gamma/\sqrt{s}$, $E_\gamma$ is the radiated photon energy in the nominal center-of-mass (CM) frame and $\sqrt{s}$ is the nominal CM energy of the collider. The quantity $s' = s(1-x)$ represents the mass squared of the final state system $f$. The radiator function $W(s,x)$ describes the energy spectrum of the virtual photon and can be computed to an accuracy better than 1%. The direction of radiated photon is peaked along the initial beams, but for $\sqrt{s} \simeq 10\,\mathrm{GeV}$ the fraction at large angle is relatively large. It has been shown a $\sim 15\%$ acceptance for these photons in BaBar.

The measurement of the corresponding leptonic process $e^+e^- \to \mu^+\mu^-\gamma$ provides the ISR luminosity. Thus, the Born cross section for a hadronic final state $\sigma_f(s')$ is given by

$$\sigma_f(s') = \frac{\Delta N_{f\gamma}\,\varepsilon_{\mu\mu}\left(1+\delta^{\mu\mu}_{\mathrm{FSR}}\right)}{\Delta N_{\mu\mu\gamma}\,\varepsilon_f\left(1+\delta^{f}_{\mathrm{FSR}}\right)}\,\sigma_{\mu\mu}(s')\,, \tag{2}$$

where $\Delta N_{f\gamma}$ ($\Delta N_{\mu\mu\gamma}$) is the number of detected $f\gamma$ ($\mu\mu\gamma$) events in the bin of width $\Delta s'$ centered at $s'$, $\varepsilon_f$ ($\varepsilon_{\mu\mu}$) is the detection efficiencies and $\delta^f_{\mathrm{FSR}}$ ($\delta^{\mu\mu}_{\mathrm{FSR}}$) is the fraction of events produced through final state radiation. The latter quantity can be sizable for the $\mu\mu$ channel, but negligible for most of the low energy hadronic states, which have vanishingly small cross sections at the nominal machine energy.

Events are tagged by detecting a photon with an energy in the CM system larger than 3 GeV. All final state particles need to be identified and detected inside the fiducial volume of the detector. The invariant mass of the hadronic final state defines the effective $e^+e^-$ CM energy $\sqrt{s'}$. A limitation of the ISR measurements is due to the much poorer mass resolution with respect to what is obtained in direct annihilation. The mass resolution can be substantially improved performing a kinematic fit requiring total energy and momentum conservation. If one or more $\pi^0$'s are expected in the final state, the kinematic fit is performed constraining also the mass of each $\pi^0$ candidate to the world average value [4].

## 2. The BaBar detector

The BaBar detector is described in detail elsewhere [5]. The information from the tracking system (Silicon Vertex Tracker and Drift Chamber) is used to measure angles and momenta of charged particles. The quartz

Cherenkov radiator (DIRC) is the main subsystem for particle identification ($K/\pi$ separation is an essential ingredient for these studies). Muons are identified in the Resistive Plate Counters installed in the magnet yoke of the BaBar solenoid, while photons are detected in the CsI calorimeter. Detector acceptances and efficiencies for the various analysis are evaluated with detailed Monte Carlo studies. Monte Carlo generators for the simulation of the hadronic final states are developed according to the approach suggested by the authors of Ref. [6]. Multiple soft-photon emission from the initial-state particles are implemented with the structure function technique [7, 8], while final state radiation is simulated by means of the PHOTOS package [9]. The accuracy of the radiative corrections is of the order of 1%.

## 3. The $\pi^+\pi^-\pi^0$ final state

The $e^+e^- \to \pi^+\pi^-\pi^0$ cross section in the energy region below the $J/\psi$ meson is usually described as the sum of four resonances: $\omega(782)$, $\phi(1020)$, $\omega' \equiv \omega(1420)$ and $\omega'' \equiv \omega(1650)$. The $\omega$ and $\phi$ parameters have been very well determined at several experiments with high statistics. On the contrary, the energy region above the $\phi$ has been studied only in two experiment: SND [10] for energies up to 1.4 GeV with statistical precision of about 10%, and DM2 [11] for energies in the $1.34 \div 2.40$ GeV range with statistical precision of about 25%. The $\omega'$ and $\omega''$ parameters are very poorly known and decay modes for these resonances are not well established.

The main goal of this analysis, whose results based on a data sample of $89\,\mathrm{fb}^{-1}$ have been recently published [12], is an independent measurement of the $e^+e^- \to \pi^+\pi^-\pi^0$ cross section, with a significant improvement in the region between 1.05 and 3.0 GeV, and the study of the two $\omega$ excitations. The $3\pi$ invariant mass spectrum is fit with a function which includes the contributions from the four vector resonances. The mass and width of $\omega(782)$ and $\phi(1020)$ mesons and the relative phase between $\omega$ and $\phi$ amplitudes are fixed to the world average values [4]. The phases of $\omega$, $\omega'$ and $\omega''$ are fixed, respectively, to $0^\circ$, $180^\circ$ and $0^\circ$. The fit result is shown along with the data in Fig. 1.

The following branching fraction products, masses and widths are obtained from the fit:

$$\begin{aligned}
\mathcal{B}(\omega \to e^+e^-)\mathcal{B}(\omega \to 3\pi) &= (6.70 \pm 0.06 \pm 0.27) \times 10^{-5},\\
\mathcal{B}(\phi \to e^+e^-)\mathcal{B}(\phi \to 3\pi) &= (4.30 \pm 0.08 \pm 0.21) \times 10^{-5},\\
\mathcal{B}(\omega' \to e^+e^-)\mathcal{B}(\omega' \to 3\pi) &= (0.82 \pm 0.05 \pm 0.06) \times 10^{-6},\\
\mathcal{B}(\omega'' \to e^+e^-)\mathcal{B}(\omega'' \to 3\pi) &= (1.3 \pm 0.1 \pm 0.1) \times 10^{-6},\\
M_{\omega'} = (1350 \pm 20 \pm 20)\ \mathrm{MeV}/c^2\,, &\qquad \Gamma_{\omega'} = (450 \pm 70 \pm 70)\ \mathrm{MeV}\,,\\
M_{\omega''} = (1660 \pm 10 \pm 2)\ \mathrm{MeV}/c^2\,, &\qquad \Gamma_{\omega''} = (230 \pm 30 \pm 20)\ \mathrm{MeV}\,.
\end{aligned}$$

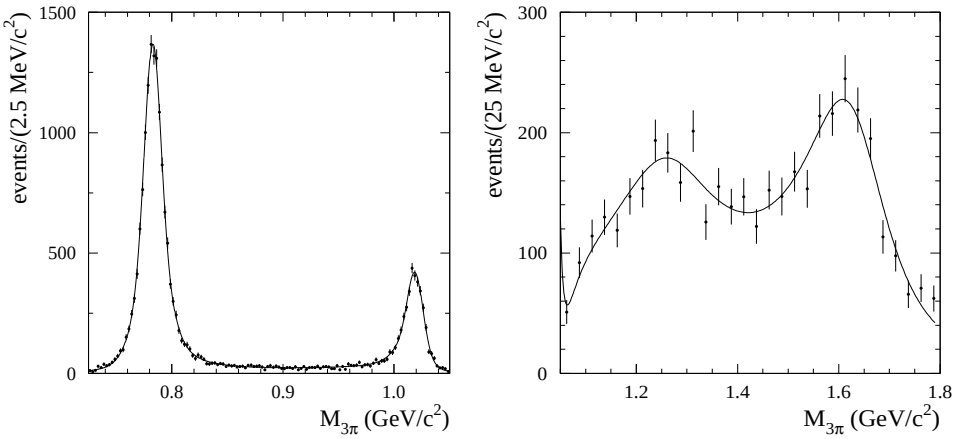


Fig. 1. Background-subtracted $\pi^+\pi^-\pi^0$ mass spectrum for masses between 0.7 and 1.05 GeV/$c^2$ (left) and between 1.05 and 1.80 GeV/$c^2$. The curves are the result of the fit described in the text (right).

Quoted errors reflect the statistical and systematic uncertainties, respectively. The results are model dependent, but can be compared to the present estimates [4]: $M_{\omega'} = 1400 \div 1450$ MeV/$c^2$, $\Gamma_{\omega'} = 180 \div 250$ MeV, $M_{\omega''} = (1670 \pm 30)$ MeV/$c^2$ and $\Gamma_{\omega''} = (315 \pm 35)$ MeV.

It should also be noticed that our measurement of the $e^+e^- \to \pi^+\pi^-\pi^0$ cross section is in agreement with data from SND, but is significantly higher than that measured by DM2 at energies above 1.4 GeV.

## 4. Final states with four charged hadrons

BaBar published results [13], based on the same data sample of 89 fb$^{-1}$ are available also for the final states with four charged hadrons, namely $\pi^+\pi^-\pi^+\pi^-$, $\pi^+\pi^-K^+K^-$and $K^+K^-K^+K^-$. The discrimination between the three final states is done on the basis of the particle identification and on the kinematic fit results for the different mass hypothesis.

No muon identification was applied since no corresponding background is expected in this sample. The background from other hadronic channels is small and is subtracted in each mass bin. Overall, more than 70000 events have been selected leading to small statistical uncertainties. The estimated systematic error is about 5% in the energy region between 1 and 3 GeV, dominated by the luminosity determination. Fig. 2 shows the derived cross section for the three final states. Our data are in good agreement with previous available results on the $4\pi$ mode. Moreover, BaBar is the only experiment which covers the entire energy range, with an accuracy

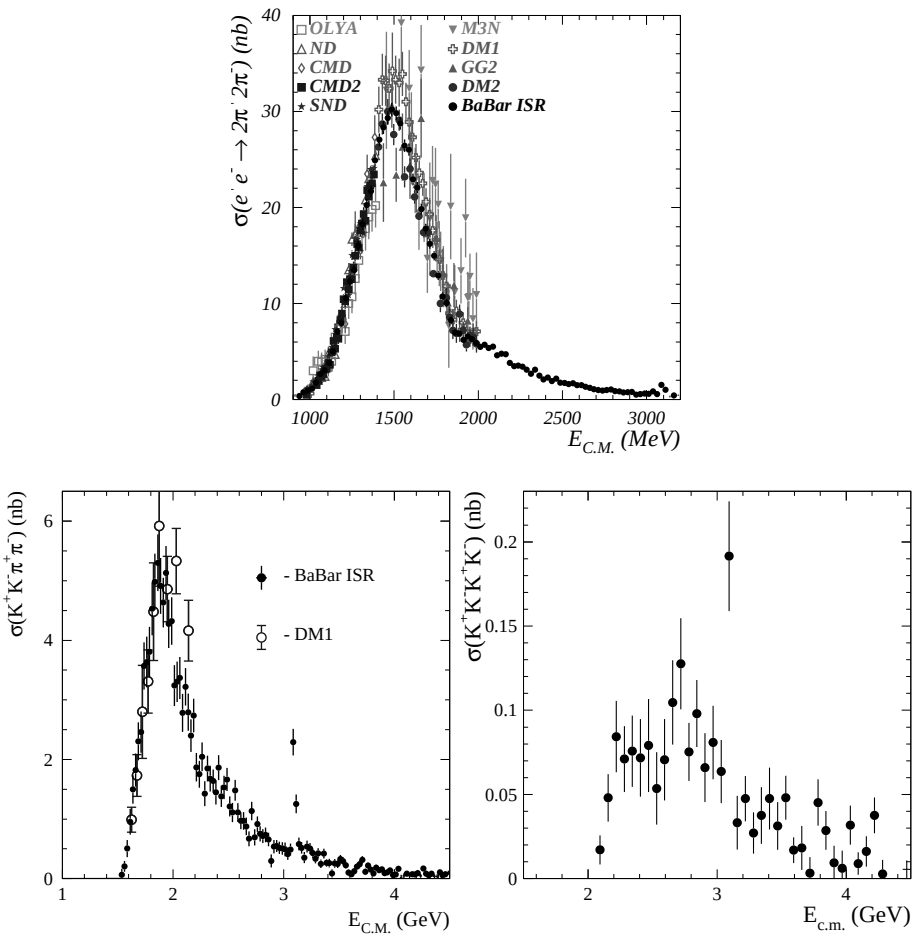


Fig. 2. $e^+e^- \to 2(\pi^+\pi^-)$, $e^+e^- \to \pi^+\pi^-K^+K^-$ and $e^+e^- \to 2(K^+K^-)$ cross section as a function of energy obtained with BaBar ISR data (black dots) in comparison with all previous $e^+e^-$ data.

comparable to the latest precise results from CMD-2 [14] and SND [15] below 1.4 GeV, and much better accuracy than older results from DCI and ADONE above 1.4 GeV. The $e^+e^- \to 4K$ has never been measured before BaBar.

The hadronic contribution to the $(g-2)_\mu$ due to the $4\pi$ mode, evaluated using all available $e^+e^-$ data in 0.56–1.8 GeV energy range, is [16] $a_\mu^{\rm hadr} = (14.21 \pm 0.87_{\rm exp} \pm 0.23_{\rm rad}) \times 10^{-10}$, while the $\tau$ data give $a_\mu^{\rm hadr} = (12.35 \pm 0.96_{\rm exp} \pm 0.40_{\rm SU2}) \times 10^{-10}$. The BaBar data in the same energy region give instead [17] $a_\mu^{\rm hadr} = (12.95 \pm 0.64_{\rm exp} \pm 0.13_{\rm rad}) \times 10^{-10}$, leading to a substantial improvement.

## 5. Final states with six hadrons

A similar analysis procedure has been applied to final states consisting of six hadrons, namely $3(\pi^+\pi^-)$, $2(\pi^+\pi^-)\pi^0\pi^0$ and $K^+K^-2(\pi^+\pi^-)$. The cross sections for the three processes, obtained with a data sample of $232\,\mathrm{fb}^{-1}$, are shown in Fig. 3. The cross section for the process $e^+e^- \to K^+K^-\pi^+\pi^-\pi^+\pi^-$ has never been measured before BaBar. The data for the $e^+e^- \to 3(\pi^+\pi^-)$ are in very good agreement with previous results, while for the $e^+e^- \to 2(\pi^+\pi^-)\pi^0\pi^0$ BaBar data show a lower cross section with respect to DM2 at energies above 1.9 GeV. A dip in the cross

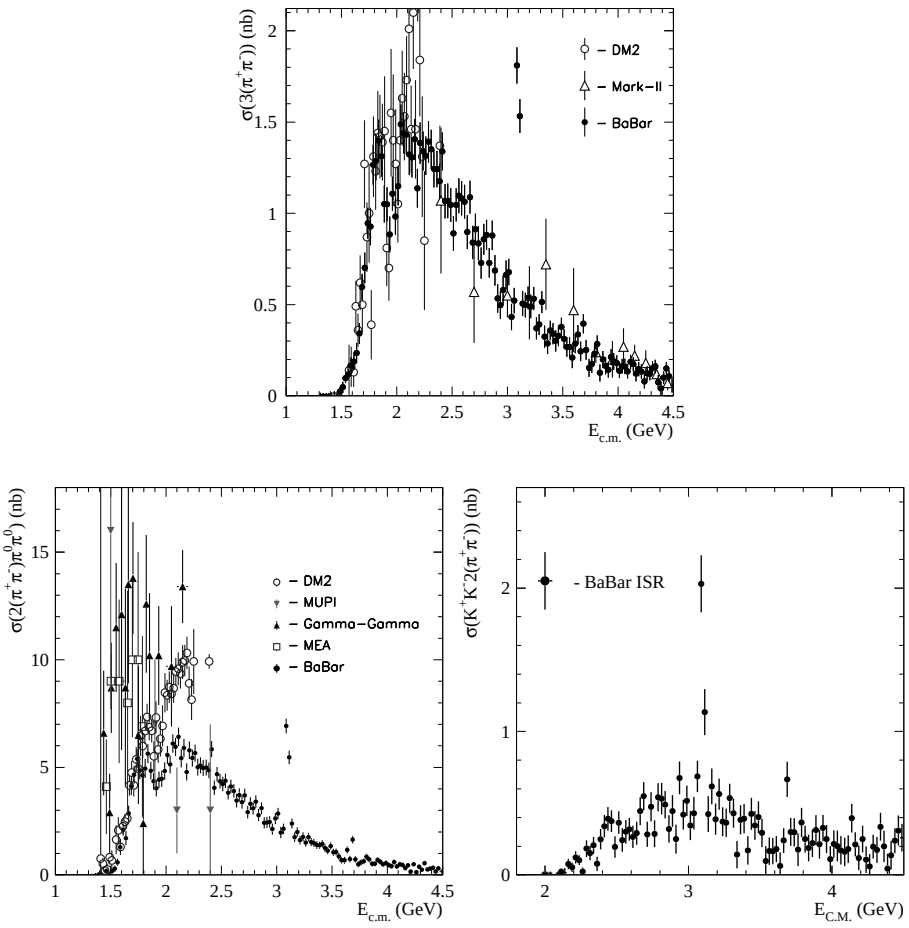


Fig. 3. $e^+e^- \to 3(\pi^+\pi^-)$, $e^+e^- \to 2(\pi^+\pi^-)\pi^0\pi^0$ and $e^+e^- \to K^+K^-2(\pi^+\pi^-)$ cross section as a function of energy obtained with BaBar ISR data (black dots) in comparison with all previous $e^+e^-$ data.

section distribution is seen around 1.9 GeV in both $6\pi$ modes. A similar structure was observed by DM2 ($e^+e^-$ annihilations) and FOCUS Collaborations (diffractive photoproduction). In order to extract the parameters of a possible resonant state sitting at 1.9 GeV, we fit both cross sections following the same procedure as in Ref. [18]. We assume a production of several interference vector states decaying to the same final state. We find:

$$\begin{aligned} m_{3\pi^+\pi^-} &= (1.88 \pm 0.03)\ \mathrm{GeV}/c^2\,, & m_{4\pi 2\pi^0} &= (1.86 \pm 0.02)\ \mathrm{GeV}/c^2\,, \\ \Gamma_{3\pi^+\pi^-} &= (0.13 \pm 0.03)\ \mathrm{GeV}\,, & \Gamma_{4\pi 2\pi^0} &= (0.16 \pm 0.02)\ \mathrm{GeV}\,, \\ \phi_{3\pi^+\pi^-} &= 21^\circ \pm 40^\circ\,, & \phi_{4\pi 2\pi^0} &= -3^\circ \pm 15^\circ\,. \end{aligned}$$

These values should be compared with results obtained by the FOCUS Collaboration [18,19]: $m = (1.91 \pm 0.01)\,\mathrm{GeV}/c^2$, $\Gamma = (0.037 \pm 0.013)\,\mathrm{GeV}$, $\phi = 10 \pm 30^\circ$.

We look at different mass combinations of the final state particles to see what structures are involved in the process. The resonant structure for the $3(\pi^+\pi^-)$ final state is surprisingly simple, considering the relatively high multiplicity of the final state, being well describe by a Monte Carlo simulation featuring only a single $\rho^0(770) \to \pi^+\pi^-$ resonance. No other resonances are observed in the $2\pi, 3\pi$ and $4\pi$ mass combinations.

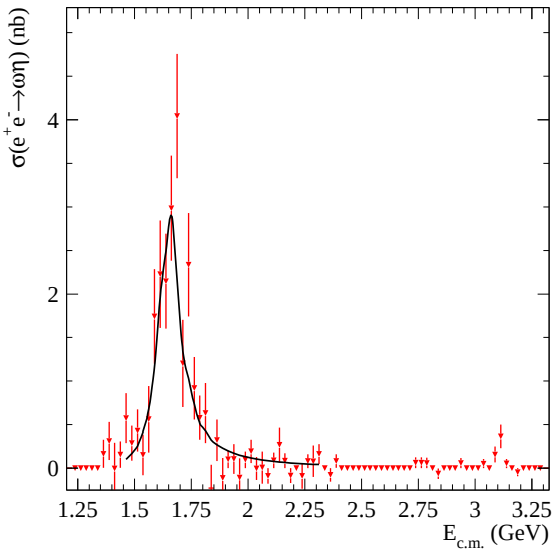


Fig. 4. $e^+e^- \to \omega\eta$ cross section as a function of energy. The line is the result of a fit to a Breit–Wigner function of the region around the peak at $\sim 1.65\ \mathrm{GeV}/c^2$. A small signal is seen also in the $J/\psi$ energy region.

A very rich resonant structure is observed instead in the $2(\pi^+\pi^-)\pi^0\pi^0$ channel, with clear signals for $\rho^0(770) \to \pi^+\pi^-$, $\rho^{\pm}(770) \to \pi^{\pm}\pi^0$ and $f_0(980) \to \pi^0\pi^0$ in the $2\pi$ combinations and signal for $\omega$ and $\eta$ decaying in $\pi^+\pi^-\pi^0$. In particular, a signal for $e^+e^- \to \omega(\pi^+\pi^-\pi^0)\ \eta(\pi^+\pi^-\pi^0)$ is also seen. The corresponding cross section distribution shows a resonant structure at $\simeq 1.65\,\mathrm{GeV}/c^2$ (see Fig. 4).

A fit of the peak region to a Breit–Wigner shape gives a resonant peak position of $(1.645 \pm 0.008)\,\mathrm{GeV}/c^2$ and a width of $(114 \pm 14)\,\mathrm{MeV}$. These values are compatible with the parameters of the $\phi(1680)$ meson, that is $m = (1.680 \pm 0.020)\,\mathrm{GeV}/c^2$ and $\Gamma = (150 \pm 50)\,\mathrm{MeV}$ [4], whose decay to $\omega\eta$ final state has never been observed. A small signal for $J/\psi \to \omega\eta$, can also be seen in Fig. 4, corresponding to 13 events after background subtraction. This signal will be used to determine the corresponding $J/\psi$ branching fraction.

## 6. The $p\bar{p}$ final state and measurement of proton form factors

The cross section for the process $e^+e^- \to p\bar{p}$ is given by

$$\sigma_{e^+e^-\to p\bar{p}} = \frac{4\pi\alpha^2 C}{3s'}\sqrt{1-\frac{2m_p^2}{s'}}\left(\left|G_{\mathrm{M}}(s')\right|^2 + \frac{2m_p^2}{s'}\left|G_{\mathrm{E}}(s')\right|^2\right), \qquad (3)$$

where $m_p$ is the mass of the proton, and $C$ is the Coulomb correction factor [20] which makes the cross section non-zero at threshold.

The ratio of electric to magnetic form factors can be extracted analyzing the distribution of the proton helicity angle in the $p\bar{p}$ rest frame. In general this distribution can be written as:

$$\frac{dN}{d\cos\theta_p} = A\left(H_{\mathrm{M}}(\cos\theta_p, s') + \left|\frac{G_{\mathrm{E}}}{G_{\mathrm{M}}}\right| H_{\mathrm{E}}(\cos\theta_p, s')\right). \qquad (4)$$

The functions $H_{\mathrm{M}}(\cos\theta_p, s')$ and $H_{\mathrm{E}}(\cos\theta_p, s')x$ do not strongly differ from the functions $1 + \cos^2\theta_p$ and $\sin^2\theta_p$, respectively. The exact expressions are obtained via Monte Carlo simulation. The mass region from $p\bar{p}$ threshold up to 3 $\mathrm{GeV}/c^2$ is divided in six intervals. For each mass bin the angular distribution after background subtraction is shown in Fig. 5. These distributions are fitted by Eq. (4), with two free parameters, $A$ and $|G_{\mathrm{E}}/G_{\mathrm{M}}|$. The functions $H_{\mathrm{E}}$ and $H_{\mathrm{M}}$ are replaced by the histograms obtained from the Monte Carlo simulation. Fig. 5 shows the result of the fits, together with the separate contribution from the two terms.

We find values of $|G_{\mathrm{E}}/G_{\mathrm{M}}|$ significantly greater than unity, as shown in Fig. 6, in disagreement with previous results from experiment PS170 at LEAR [21]. We should note, however, that PS170 data were affected

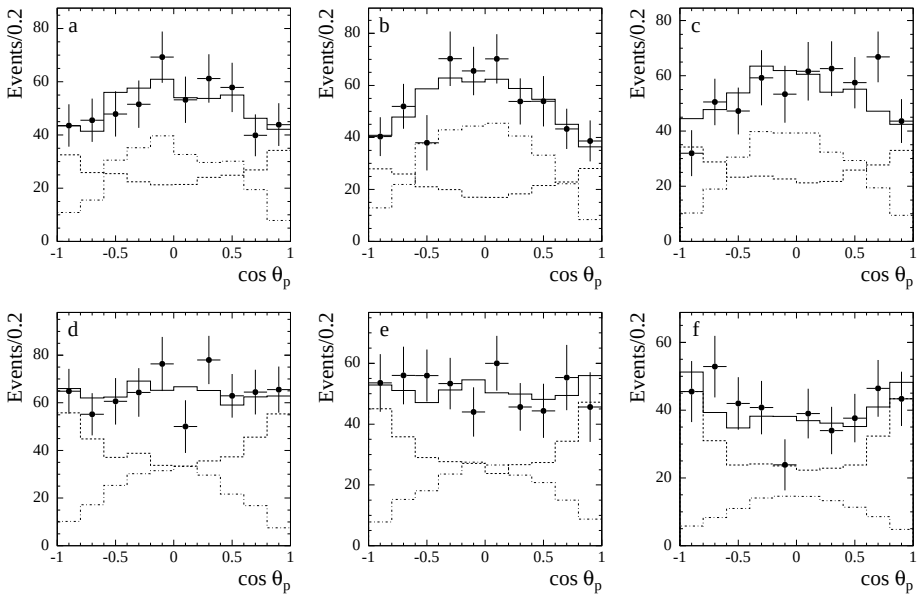


Fig. 5. Distributions of the proton helicity angle in the $p\bar{p}$ rest frame for different invariant mass regions. From plot "a" to "f", the energy regions are, respectively, 1.877–1.950 GeV/$c^2$, 1.950–2.025 GeV/$c^2$, 2.025–2.100 GeV/$c^2$, 2.100–2.200 GeV/$c^2$, 2.200–2.400 GeV/$c^2$and 2.400–3.000 GeV/$c^2$. The points with errors are the background-subtracted data, the solid histogram is the fit result and the dashed and dot-dashed histograms show the separate contributions of the terms corresponding to magnetic and electric form factors, respectively.

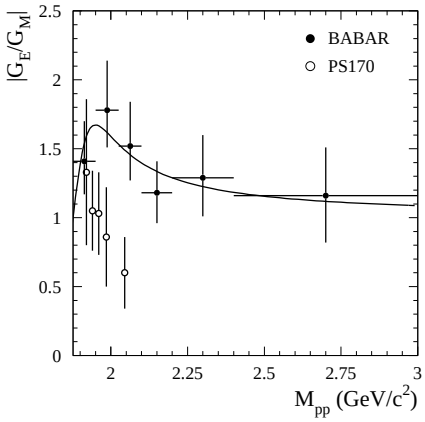


Fig. 6. The ratio $|G_{\rm E}/G_{\rm M}|$ measured by BaBar as a function of the $p\bar{p}$ mass (filled circles). The line is the result of the fit of BaBar data. For comparison, previous data from PS170 experiment are shown (open circles).

by strong angular dependence of the detection efficiency, while one of the advantages of ISR technique over conventional $e^+e^-$ and $p\bar{p}$ experiments is just that the detection efficiency is very weakly dependent on invariant mass and angular distributions.

The $e^+e^- \to p\bar{p}$ cross section, $\sigma_{p\bar{p}}(s')$, is measured up to an invariant mass $s' \simeq 4.5$ GeV/$c^2$. We extract from the cross section measurement the so called "effective form factor", defined as

$$\left|F_p(s')\right| = \sqrt{\sigma_{p\bar{p}}(s')/\sigma_0(s')}\,, \tag{5}$$

where $\sigma_0(s')$ is the normalization cross section obtained from Eq. (3) under the assumption $|G_{\rm E}| = |G_{\rm M}| = 1$. As seen above, this assumption is not supported by our data, anyway it allows to compare our measurement with data from previous experiments, both $e^+e^-$ and $p\bar{p}$, as it is reported in Fig. 7. We observe rapid decrease of both the form factor and the cross section near to 2.25 and 3 GeV/$c^2$, which have been essentially never discussed in literature. The form factor distribution presents also a steep behavior near threshold, as already observed by the PS170 experiment. This enhancement of the form factor at threshold is also of difficult interpretation, but it could be a hint of the presence of a barion–antibarion resonance below the $p\bar{p}$ threshold. This interpretation is supported also by the observation of similar behavior in other processes involving different dynamics: for example the distribution of the invariant mass of the $p\bar{p}$ couple in the decay $B \to Kp\bar{p}$ shows a similar enhancement at threshold.

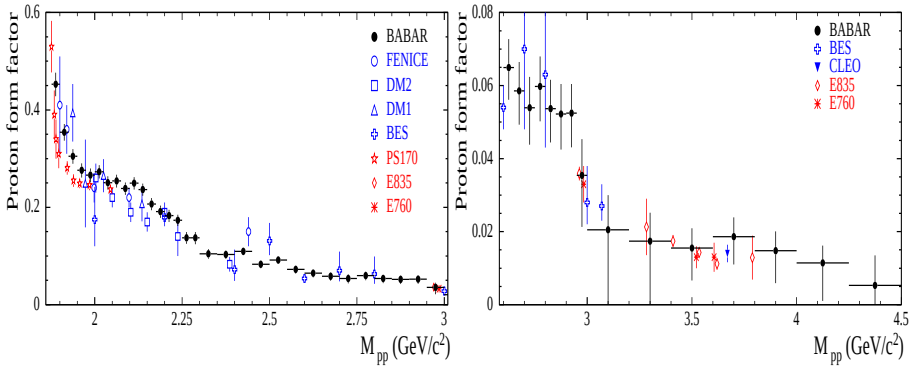


Fig. 7. Proton form factor measured by BaBar (black dots) compared to results from previous $e^+e^-$ and $p\bar{p}$ experiments.

## 7. The $J/\psi$ and $\psi(2S)$ decays

The differential cross section for a ISR production of a narrow resonance (vector meson $V$), decaying into a final state $f$, is given by

$$\frac{d\sigma(s,\theta)}{d\cos\theta} = \frac{12\pi^2\Gamma(V\to e^+e^-)\mathcal{B}(V\to f)}{m_V s}\, W(s,x_0,\theta)\,, \tag{6}$$

where $m_V$ and $\Gamma(V\to e^+e^-)$ are the mass and electronic width of the vector meson $V$, $\mathcal{B}(V\to f)$ is the branching fraction of $V$ into the final state $f$ and $x_0 = 1 - m_v^2/s$. Therefore, the measurement of the cross section for production of a certain final state $f$ in the $J/\psi$ and $\psi(2S)$ energy region allows to determine the quantities $\Gamma(J/\psi\to e^+e^-)\mathcal{B}(J/\psi\to f)$ and $\Gamma(\psi(2S)\to e^+e^-)\mathcal{B}(\psi(2S)\to f)$.

Clear signal for both $J/\psi$ and $\psi(2S)$ has been observed in most of the final states presented in this note. Using the world average values for the $J/\psi$ and $\psi(2S)$ electronic width and for $\mathcal{B}(J/\psi\to\mu^+\mu^-)$, we extract the $J/\psi$ and $\psi(2S)$ branching fractions listed in Table I and compared to the previous estimates [4]. It can be noted that our measurements generally agree with previous results, giving in several cases much more accurate

TABLE I

Summary of $J/\psi$ and $\psi' \equiv \psi(2S)$ branching fractions measurements.

| Mode | BaBar | PDG 2004 |
|---|---|---|
| $\mathcal{B}(J/\psi\to\pi^+\pi^-\pi^0)$ | $(2.18\pm0.19)\times10^{-2}$ | $(1.50\pm0.20)\times10^{-2}$ |
| $\mathcal{B}(J/\psi\to\pi^+\pi^-\pi^+\pi^-)$ | $(3.61\pm0.26\pm0.66)\times10^{-3}$ | $(4.0\pm1.0)\times10^{-3}$ |
| $\mathcal{B}(J/\psi\to K^+K^-\pi^+\pi^-)$ | $(6.2\pm0.5\pm0.5)\times10^{-3}$ | $(7.2\pm2.3)\times10^{-3}$ |
| $\mathcal{B}(J/\psi\to K^+K^-K^+K^-)$ | $(7.4\pm1.2\pm1.2)\times10^{-4}$ | $(9.2\pm3.3)\times10^{-4}$ |
| $\mathcal{B}(J/\psi\to 3(\pi^+\pi^-))$ | $(4.40\pm0.29\pm0.29)\times10^{-3}$ | $(4.0\pm2.0)\times10^{-3}$ |
| $\mathcal{B}(J/\psi\to 2(\pi^+\pi^-)\pi^0\pi^0)$ | $(1.65\pm0.10\pm0.18)\times10^{-2}$ | n.a. |
| $\mathcal{B}(J/\psi\to K^+K^-2(\pi^+\pi^-))$ | $(5.09\pm0.42\pm0.35)\times10^{-3}$ | $(3.1\pm1.3)\times10^{-3}$ |
| $\mathcal{B}(J/\psi\to\phi\ 2(\pi^+\pi^-))$ | $(1.77\pm0.35\pm0.12)\times10^{-3}$ | $(1.60\pm0.32)\times10^{-3}$ |
| $\mathcal{B}(J/\psi\to\omega\eta)$ | $(1.47\pm0.41\pm0.15)\times10^{-3}$ | $(1.58\pm0.16)\times10^{-3}$ |
| $\mathcal{B}(J/\psi\to p\bar{p})$ | $(2.22\pm0.16)\times10^{-3}$ | $(2.12\pm0.10)\times10^{-3}$ |
| $\mathcal{B}(\psi'\to J/\psi\pi^+\pi^-)$ | $0.361\pm0.015\pm0.028$ | $0.317\pm0.011$ |
| $\mathcal{B}(\psi'\to 2(\pi^+\pi^-)2\pi^0)$ | $(5.3\pm1.6\pm0.6)\times10^{-3}$ | n.a. |
| $\mathcal{B}(\psi'\to K^+K^-2(\pi^+\pi^-))$ | $(2.1\pm1.0\pm0.2)\times10^{-3}$ | n.a. |
| $\mathcal{B}(\psi'\to p\bar{p})$ | $(3.3\pm0.9)\times10^{-4}$ | $(2.07\pm0.31)\times10^{-4}$ |

estimates or representing the first measurement ever. It is interesting to notice that our measurement $\mathcal{B}(J/\psi \to 3\pi) = (2.18 \pm 0.19)\%$ is in substantial disagreement with the PDG value of $(1.47 \pm 0.13)\%$, but it is in very good agreement with the recent result from BES Collaboration [23], $\mathcal{B}(J/\psi \to 3\pi)_{\rm BES} = (2.10 \pm 0.12)\%$.

## 8. Conclusions

The recent results obtained by BaBar study hadronic final states produced through ISR demonstrate the high physics potential of this sample, which yields precise measurements of $e^+e^-$ annihiliation cross sections. A very rich program can be exploited in BaBar with this technique: spectroscopy, form factor measurements, search for exotic states, *etc.* Besides, measurements of exclusive hadronic channels constitute the main approach for measuring $R = \sigma(e^+e^- \to \text{hadrons})/\sigma(e^+e^- \to \mu^+\mu^-)$, providing input for theoretical determination of the hadronic contribution to $(g-2)_\mu$ and $\alpha(M_Z^2)$.

Cross section measurements for $e^+e^- \to 3\pi, 4\pi, 6\pi, 2K2\pi, 4K, 2K4\pi$, from threshold up to 4.5 GeV, have been presented in this note. The systematic uncertainties are at the level of those of direct $e^+e^-$ experiments, but the collected samples have better statistical significance, expecially in the energy region between 1.4 and 3 GeV.

We have also measured the $e^+e^- \to p\bar{p}$ cross section, together with the angular distribution for the final state. We extract from these measurement precise determination of the ratio of the electric to magnetic proton form factor, $|G_{\rm E}/G_{\rm M}|$, and of the effective form factor in the energy range from threshold up to 4.5 GeV. We find a value of $|G_{\rm E}/G_{\rm M}|$ significantly greater than unity and confirm the rapid growth of the effective form factor near threshold, already observed in previous experiments.

The radiative return to $J/\psi$ and $\psi(2S)$ resonances allows precise measurements of several branching fractions products.

I wish to thank the organizers of the XXIX International Conference of Theoretical Physics, "Matter to the Deepest" for the kind hospitality at Ustroń. The author and the whole BaBar Collaboration are grateful for the extraordinary contributions of the PEP-II colleagues in achieving the excellent luminosity and machine conditions that have made this work possible. This work is supported by DOE and NSF (USA), NSERC (Canada), IHEP (China), CEA and CNRS-IN2P3 (France), BMPF and DFG (Germany), INFN (Italy), FOM (The Netherlands), NFR (Norway), MIST (Russia) and PPARC (United Kingdom). Individuals have received support from CONACyT (Mexico), the A.P. Sloan Foundation, the Research Corporation, and the Alexander von Humboldt Foundation.

## REFERENCES


[1] A.B. Arbuzov *et al.*, *J. High Energy Phys.* **9812**, 009 (1998).

[2] S. Binner, J.H. Kuhen, K. Melnikov, *Phys. Lett.* **B459**, 279 (1999).

[3] M. Benayoun *et al.*, *Mod. Phys. Lett.* **A14**, 2605 (1999).

[4] S. Eidelman *et al.*, Review of Particle Physics, *Phys. Lett.* **B592**, 1 (2004).

[5] B. Aubert *et al.*, BaBar Collaboration, *Nucl. Instrum. Methods* **A479**, 1 (2002).

[6] H. Czyż, J.H. Kühn, *Eur. Phys. J.* **C18**, 497 (2001).

[7] A.B. Arbuzov *et al.*, *J. High Energy Phys.* **9710**, 001 (1997).

[8] M. Caffo, H. Czyż, E. Remiddi, *Nuovo Cim.* **A110**, 515 (1997); *Phys. Lett.* **B327**, 369 (1994).

[9] E. Barberio, B. van Eijk, Z. Wąs, *Comput. Phys. Commun.* **66**, 115 (1991).

[10] M.N. Achasov *et al.*, SND Collaboration, *Phys. Rev.* **D66**, 032001 (2002).

[11] A. Antonelli *et al.*, *Z. Phys.* **C56**, 15 (1992).

[12] B. Aubert *et al.*, *Phys. Rev.* **D70**, 072004 (2004).

[13] B. Aubert *et al.*, *Phys. Rev.* **D71**, 052001 (2005).

[14] R.R. Akhmetshin *et al.*, CMD-2 Collaboration, *Phys. Lett.* **B466**, 392 (1999); *Phys. Lett.* **B475**, 190 (2000).

[15] M.N. Achasov *et al.*, SND Collaboration, *J. Exp. Theor. Phys.* **96**, 789 (2003).

[16] M. Davier, S. Eidelman, A. Hoecker, Z. Zhang, *Eur. Phys. J.* **C31**, 503 (2003).

[17] M. Davier, `hep-ex/0312063`.

[18] P.L. Frabetti *et al.*, E687 Collaboration, *Phys. Lett.* **B514**, 240 (2001).

[19] P.L. Frabetti *et al.*, E687 Collaboration, *Phys. Lett.* **B578**, 290 (2004).

[20] C. Tzara, *Nucl. Phys.* **B18**, 246 (1970).

[21] G. Bardin *et al.*, PS170 Collaboration, *Nucl. Phys.* **B411**, 3 (1994).

[22] V.L. Chernyak, A.R. Zhitnistsky, *JETP Lett.* **25**, 510 (1977); G. Lepage, S. Brodsky, *Phys. Rev. Lett.* **43**, 545 (1979).

[23] J.Z. Bai *et al.*, BES Collaboration, *Phys. Rev.* **D70**, 012005 (2004).